11-1-2017

Catalytic Reduction of Bisulfite by Myoglobin/Surfactant Films

Radalla Abdellatty
Marquette University

Md. Hafizur Rahman
Marquette University

Michael D. Ryan
Marquette University, michael.ryan@marquette.edu

Accepted version. *Electroanalysis*, Vol. 29, No. 11 (November 2017): 2437-2443. DOI.

Electroanalysis, Vol. 29, No. 1 (date): 2437-2443. DOI.

Catalytic Reduction of Bisulfite by Myoglobin/Surfactant Films

Radalla Abdelatty, Md.
Marquette University, Chemistry Department, PO Box 1881, Milwaukee, WI 53201 USA

Hafizur Rahman
Marquette University, Chemistry Department, PO Box 1881, Milwaukee, WI 53201 USA

Michael D. Ryan
Marquette University, Chemistry Department, PO Box 1881, Milwaukee, WI 53201 USA

Abstract
The voltammetry of bisulfite at a film formed with myoglobin was studied in aqueous solutions. A broad wave was observed for the reduction of bisulfite. Using controlled potential electrolysis, the reduction at potentials positive of the Fe^{II}/Fe^{I} wave formed dithionite exclusively. As the potential approached the region for the Fe^{II}/Fe^{I} reduction, bisulfite was reduced primarily to HS^-. Even at the negative potentials, some dithionite was still formed, which could then be electrochemically reduced to thiosulfate. Analysis of the formation of HS^-, dithionite and thiosulfate during the electrolysis was consistent with the parallel formation of HS^- and dithionite, the latter of which was reduced to thiosulfate. Thiosulfate was verified by chemical analysis of the products from controlled potential electrolysis of the solution, and dithionite was observed spectroscopically using spectroelectro-chemistry.

Keywords
bisulfite, myoglobin, electrocatalytic, film

1. Introduction

A class of enzymes called sulfite reductases catalyzes the reduction of bisulfite in nature. These enzymes fall into two broad classes: dissimilatory and assimilatory sulfite reductases. These enzymes have been reviewed by Grein et al [1] and Simon and Kroneck [2]. The largest group of sulfite reductases contain a siroheme and 4Fe-4S cluster in close proximity [1]. Crane et al. [3] probed the catalytic mechanism by determining the x-ray structure of *E. coli* sulfite reductase hemoprotein which was bound by various substrates including bisulfite and sulfite. Parey et al. [4] used a similar approach with the dissimilatory sulfite reductase from *A. fulgidus*. From their work, they proposed a catalytic cycle which involved a series of $2H^+/2e^-$ reduction steps starting with bisulfite and ending with S^{2-}, a mechanism previously proposed by Tan and Cowan [5]. The two proposed intermediates S(II) and S(I) remained coordinated to the siroheme iron during catalytic cycle. Silaghi-Dumitrescu and Makarov [6] examined the redox cycle using the DFT approach, using the cycle proposed by Crane et al. [3] (Scheme 1, coordination by 4Fe-4S cluster has been omitted for clarity of presentation).

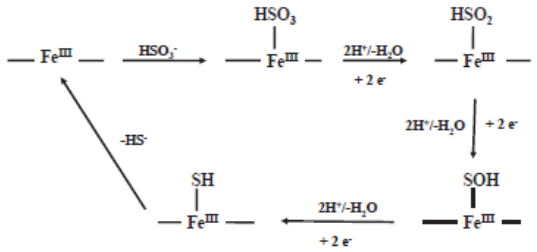

Scheme 1. Reduction mechanism for sulfite reduction based on the sulfite reductase mechanism [3, 6].

While the assimilatory nitrite reductases reduce bisulfite to sulfide, the mechanism for some dissimilatory sulfite reductases is more complex. The catalytic unit is a heterodimer, DsrAB, which is bound to a third protein, DsrC [7]. This latter protein forms a trisulfide species during sulfite reduction [8]. For the assimilatory enzyme, hydrogen sulfide is used for the synthesis of sulfur containing amino acids.

The direct voltammetric reduction of bisulfite at a gold electrode leads to dithionite [9]:

$$2HSO_3^- + 2H^+ + 2e^- \rightarrow S_2O_4^{2-} + 2H_2O \qquad (1)$$

Detailed voltammetric and coulometric studies supported the following mechanism:

$$SO_2 + 2\,H^+ + 2\,e^- \rightarrow H_2SO_2 \qquad (2)$$

$$H_2SO_2 + HSO_3^- \rightarrow S_2O_4^{2-} + H^+ + H_2O \qquad (3)$$

$$HSO_2^- + HSO_3^- \rightarrow S_2O_4^{2-} + H_2O \qquad (4)$$

Elemental sulfur and thiosulfate can also be formed from the disproportionation of dithionite [10]. The catalytic reduction of bisulfite by a water-soluble iron porphyrin was report by Kline et al. [11]. Yields of H_2S were reported to be 52% at pH 3.5, but the yields of other products were not reported.

Limited studies of model iron porphyrin complexes with SO_2 and related oxysulfur species have been reported.

Scheidt et al.[12] and Reynolds and Holm[13] have reported no isolatable SO_2 adducts between SO_2 and Fe^{II}-porphyrins. Both observed the oxidation of SO_2 to sulfate (bisulfate) which was coordinated to the ferric complex. Kuroi and Nakamoto also observed no complexes between SO2 and ferrous porphyrins at room temperature, but an SO_2 adduct was observed at 20K in an argon matrix[14]. Fe(II)-porphyrin-SO_2 adducts were observed under reducing conditions where the Fe(II) porphyrin was reacted with SOCl2 in the presence of benzene/zinc dust[15]. While the SO_2 adduct was not isolated, the visible and infrared spectra were consistent with such a species. The reducing conditions prevented the oxidation of the ferrous species.

Surfactant films have been shown to be quite effective in enhancing the electron transfer rates between the electrode and proteins such as myoglobin[16]. De Groot et al.[17] showed that the heme was probably extruded in the film. This was later disputed by Guto and Rusling[18], but Sagara et al.[19] supported the conclusions of De Groot. Their data were consistent with heme release by conformation change caused by DDAB. Lee and Bond later studied myoglobin and heme in DDAB and found conditions under which the heme was not extruded in the film[20]. Myoglobin in surfactant films such as DDAB can be reduced reversibly in two one-electron steps. The first step is the Fe(III)/Fe(II) reduction, while the second step involves the formation of Fe(I)[21]. These films have been used by Lin et al.[22] to catalyze the reduction of nitrite by myoglobin. A variety of products were formed, including ammonia, hydroxylamine and nitrous oxide. Chen and Tseng[23] reduced bisulfite electrocatalytically using a hemoglobin/DDAB film, though the details of that reaction were not studied extensively. A better understanding of the reduction mechanism can be obtained though if the evolution of the reduction products can be investigated. As a result, the voltammetric, coulometric and spectroelectrochemical reduction of bisulfite, using a myoglobin created film as a catalyst was initiated in our laboratory and is reported in this work.

2. Experimental

2.1. Materials and solutions

Horse skeletal muscle myoglobin from Sigma Chemical Co. was dissolved in a pH 7.3 Tris buffer solution containing 50 mM KBr. Didodecyldimethyl ammonium bromide (DDAB, 99%) was obtained from Acros. Sodium bisulfite anhydrous was obtained from Sigma (99%), and used as obtained. The buffers were Tris (pH 7.3), phthalate (pH 5), phosphate (pH 6), and borate (pH 9). The pH of the buffers was adjusted with HCl or NaOH solutions. The supporting electrolyte were

0.1M KCl or 0.05 M KBr. All other chemicals were of analytical grade. The water was purified by a Nanopure System to a specific resistance (> 15 M□-cm).

The working electrode was a DDAB/myoglobin modified glassy carbon electrode. The electrode was polished to remove any previous adsorbed layers and to regenerate the bare surface. Just before modification, the electrode was rinsed with distilled water in a sonicator and treated with a 1:3:4 (v/v/v) solution of concentrated HNO_3-HCl-H_2O for 1015 min in order to roughen the electrode so as to increase the amount of the immobilized biocatalyst. A 46 mg sample of DDAB was dispersed in 10 mL distilled water and ultrasonicated for at least 6 hr in order to obtain a clear solution. A 80 mg sample of myoglobin, 9.7 mg of Trizma base and 66 mg of Trizma HCl (Sigma-Aldrich Chemical Co.) was dissolved in 10 mL of distilled water (0.5 mM myoglobin and pH 7.3 Tris buffer). A 2 µL DDAB aliquot and a 2 µL myoglobin solution was spread onto the glassy carbon electrode. After use, it could be stored in air or buffer at room temperature.

2.2.Voltammetry.

A BAS rotating electrode, RDE-2, was connected to a Cypress System potentiostat. Controlled potential electrolyses and linear sweep voltammetric (LSV) data were collected with a CS-1200 Cypress System

potentiostat. A three-electrode cell was used for the experiment. The working electrodes were a Mb/DDAB modified glassy carbon electrode. A semi-micro Ag/AgCl (saturated KCl) and a platinum disk (Cypress Systems) were used as reference and auxiliary electrodes, respectively. All solutions were purged with dinitrogen gas, which was also used for stirring the electrolysis solutions. For LSV experiments, the scan rate was 10 mV/s and the rotation rate was 1000 rpm.

2.3. Spectroelectrochemistry.

The UV/visible data were obtained with a Hewlett-Packard 8452A diode array spectrophotometer. An optically transparent thin layer electrode (OTTLE) cell was used for the spectroelectrochemical studies. Films were prepared by depositing a few tens of microliters of Mb/DDAB in pH 7.3 Tris buffer onto the surface of gold coated OTTLE glass slide, which was dried overnight. The auxiliary electrode was a platinum mesh which was sealed with silver epoxy. A Ag/AgCl (saturated KCl) reference electrode was inserted into the OTTLE cell. The cell was placed in the sample compartment, and a blank scan was taken. The evolution of the spectra of Mb/DDAB films with potential was recorded in buffer solutions containing 50 mM KBr both in the absence and presence of bisulfite. All the spectroelectrochemical experiments were carried out under a dinitrogen atmosphere, and were purged for at least 30 minutes prior to the initiation of the experiment. Infrared (IR) samples were prepared as KBr pellets and the spectra obtained with a Nicolet infrared spectrophotometer.

2.4. Bulk Electrolysis.

Controlled-potential electrolysis of bisulfite in buffer solutions with different pH values at -600 and –1100 mV were done in the spectroelectrochemical cell using a Mb/DDAB film on gold coated OTTLE glass slide. Reduction products and the bisulfite concentrations were measured at different times during the electrolysis.

2.5.Determination of Reduction Products.

The concentrations of dithionite and thiosulfate in the coulometric solutions were determined using the UV absorbance at 316 and 220 nm, respectively, using standard solutions. The phenanthroline method [24] was used to determine the concentrations of bisulfite by removing aliquots of solution during the electrolysis. The concentration of sulfide was determined potentiometrically using a sulfide selective electrode. Details of the analytical procedure are given in the Supporting Information.

The concentration of dithionite was also determined voltammetrically. The cell was filled with 5.0 mL of 20 mM bisulfite in the buffer with an ionic strength of 0.1 M, adjusted with KCl. The solution was degassed with dinitrogen and the electrolysis carried out at a glassy carbon modified Mb/DDAB electrode at -600 mV. After the desired electrolysis time, 5.0 mL of 0.1 M NaOH was added anaerobically, and the linear sweep scan at a uncoated glassy carbon electrode was initiated [25]. A wave for dithionite was observed, and the concentration determined from a calibration curve.

3. Results and Discussion.

3.1. Catalytic Reduction of bisulfite at Mb/DDAB Films

Films were made using myoglobin and hemin. It was found that myoglobin films were easier to make and were more reproducible. While we will refer to myoglobin films in this work, it is most probable that the heme was extruded, and the catalysis was carried out by the heme group itself. The reduction of myoglobin (Mb) films in a didodecyl dimethyl ammonium bromide (DDAB) surfactant gave rise to a pair of well-defined, quasi-reversible cyclic voltammetric redox peaks at -0.36 V and -1.22 V vs. Ag/AgCl in pH 7.0 phosphate buffer (Figure 1), which was consistent with previous work. The first wave was characteristic of the Fe^{III}/ Fe^{II} redox couple, while the second wave corresponded to the Fe^{II}/Fe^{I} redox couple (similar results were obtained with both myoglobin and

hemin films). The current function for both these waves followed the behavior of a surface adsorbed species with the peak current being proportional to scan rate.

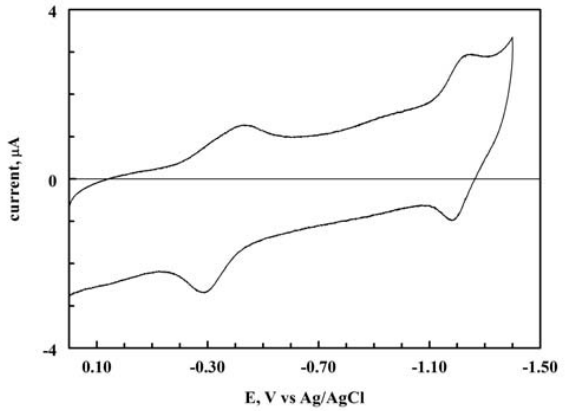

Fig. 1. Cyclic voltammograms of myoglobin-DDAB modified glassy carbon electrode in the absence of bisulfite.

Rotating disk voltammetry of the Mb-DDAB modified film in the presence of bisulfite is shown in Figure 2. In the presence of bisulfite, current at the first wave was unaffected (current too small to be observed in the RDE voltammetry). At the second wave though, the limiting current increased significantly and shifted to more positive potentials. These results were typical of a catalytic mechanism involving a species in solution. The second wave showed the presence of two overlapping waves, indicating that the reduction mechanism might be potential dependent.

The limiting current for the second wave was independent of rotation rate (between 50 and 300 rpm) but increased linearly with the concentration of bisulfite (Figure 2).

The following mechanism can be postulated for the reaction of bisulfite with Mb/hemin in the film at the limiting current region:

$$Fe^{III} + e^- \rightarrow Fe^{II} \qquad (5)$$

$$Fe^{II} + e^- \rightarrow Fe^{I} \qquad (6)$$

$$Fe^{I} + HSO_3^- \rightarrow Fe^{III} + \text{products} \qquad (7)$$

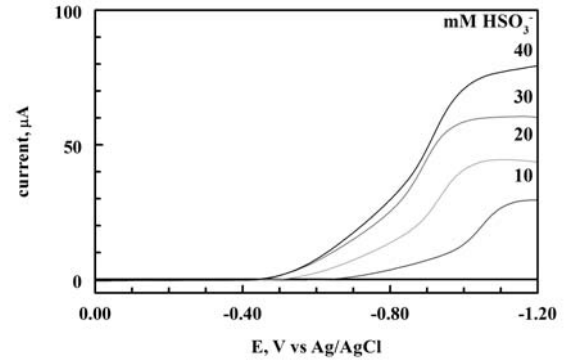

Fig. 2. Rotating disk voltammogram of a myoglobin-DDAB modified carbon electrode in the presence of bisulfite. Rotation rate = 100 rpm.

Similar curves can be obtained using cyclic voltammetry, and the peak current was found to be proportional to the bisulfite concentrations for [HSO_3^-] < 10 mM (Figure 3). This was consistent with the work of using a related protein (hemoglobin) [23]. This aspect of the electrochemistry of the reduction of bisulfite at a DDAB/myoglobin film was not investigated further. At higher concentrations, there was a loss of linearity.

Complete analysis of the voltammetric data for the electrocatalytic reduction of bisulfite at Mb-DDAB modified films requires a determination of the ultimate products of the reduction. The catalytic current was pH dependent, as shown in Figure 4. The insert shows the plateau current as a function of pH, with a pK_a = 7.3, which is the pK_a of the second dissociation of sulfurous acid. The catalytic current was found to be proportional to the equilibrium concentration of bisulfite.

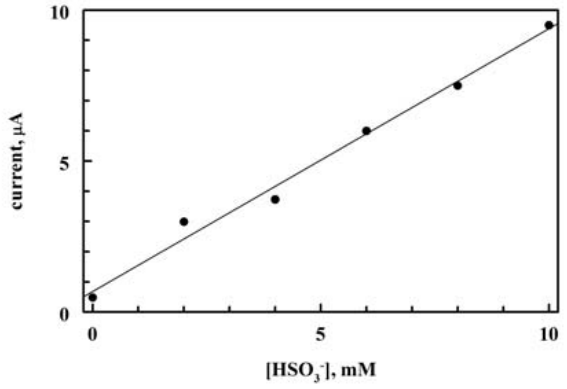

Fig. 3. The peak current as a function of bisulfite concentration before the saturation level of the film for a Mb-DDAB modified glassy carbon electrode in pH 7.3 tris buffer and 0.10 M KCl ionic strength at scan rate 50 mV/s.

Bulk electrolysis (controlled potential coulometry) at a potential more negative than the $MbFe^{II}/Fe^{I}$ potential (-1100 mV vs. Ag/AgCl) for bisulfite solutions at pH 5 containing 100 mM KCl as a constant ionic strength at room temperature was carried out at Mb-DDAB modified films on a carbon electrode. The current decayed exponentially with time as expected for a diffusion/convection controlled electrolysis.

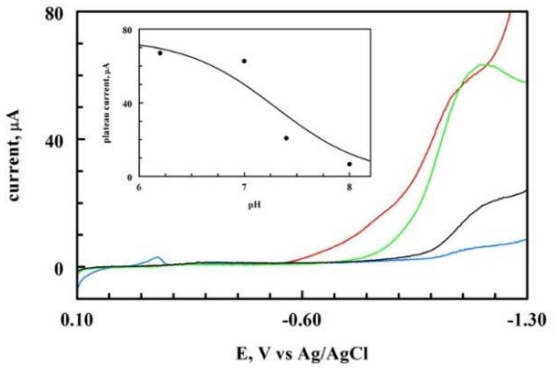

Fig. 4. Catalytic current for the reduction of bisulfite as a function of pH. Catalytic current = Observed current – current without bisulfite. pH 6.2 (red); pH 7.0 (green); pH 7.4 (black); pH 8.0 (blue). Insert: catalytic current at -1.20 V vs pH.

During the electrolysis, aliquots were also removed and the electrolysis products were detected using a sulfide selective electrode, as described in the Experimental Section. Bisulfide, HS^-, was the main electrolysis product at -1100 mV vs. Ag/AgCl, according to the following reaction:

$$HSO_3 + 6\ H^+ + 6\ e^- \longrightarrow HS^- + 3\ H^2O \qquad (8)$$

The concentration of the product, HS^-, was followed up to two hours, and the results are shown in Figure 5. The yield of the bisulfide, HS^-, was 60%. These results were similar to the results obtained by Kline et al. [11] for a water-soluble iron porphyrin. They also observed less than stoichiometric amounts of HS^- (52%).

The variation in the concentration of bisulfide, HS^-, with time showed first order reaction kinetics typical for controlled potential electrolysis. The solid line was the best-fit line for a first order reaction kinetics ($p = 0.040\ s^{-1}$, where $p = m_{HSO3}\ A/V$; m_{HSO3} is the mass diffusion coefficient, A = area of the electrode, V = volume of the solution) for the disappearance of $HSO3^-$. The rate of appearance of HS^- and $S_2O_3^{2-}$ followed the same rate constant, indicating that these species were formed at the same rate as bisulfite was consumed. Dithionite, though, disappeared rapidly after its formation due to its further reduction to thiosulfate. All the theoretical lines in Figure 5 were drawn using the theory of Bard and Mayell [26] with p (coulometric parameter) equal to $0.040\ s^{-1}$ and the overall yields of HS^- (60%) and thiosulfate (35%). The line for the disappearance of dithionite was insensitive to the rate of the dimerization reaction (SO2 to dithionite) and depended only on p. The reduction of dithionite to thiosulfate is given by Eq. 9.

$$S_2O_4^{2-} + 2\ H^+ + 2\ e^- \rightarrow S_2O_3^{2-} + H_2O \qquad (9)$$

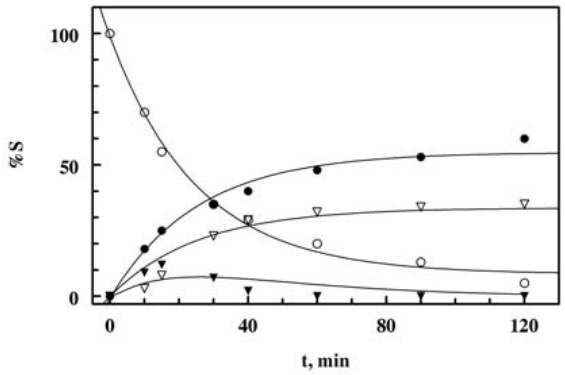

Fig. 5. Sulfur containing reactants and products as a function of time for controlled potential electrolysis of 20 mM bisulfite at pH 5.0 and at -1100 mV. $HSO3^-$ (○); HS^- (●); $S2O3^{2-}$ (▽); $S2O4^{2-}$ (▼). Solid lines correspond to first order kinetics, or consecutive first order reactions for dithionite.

The lag between the formation of dithionite and its conversion to thiosulfate can been seen in Figure 5. Early in the electrolysis, the dithionite concentration followed the thiosulfate trend line, while the thiosulfate concentration was less than expected. As time proceeded, dithionite, which was formed by the dimerization of the $SO2^-$ radical, was reduced to thiosulfate. At potentials before the formation of Fe^I, only the one-electron product ($SO2^-$ radical) is formed, which rapidly dimerizes when it dissociates from the iron. At more negative potentials, the one-electron reduced species can be bypassed, and multi-electron reduction can occur. Based on the DFT studies of sulfite reductase by Silaghi-Dumitrescu and Makarov [6], these species will remain coordinated to the iron. At this time, though, model studies of these species are very limited. Even in the potential region where Fe^I is formed, the one-electron reduction product (dithionite) is significant.

The yield of HS^- was dependent upon pH, as shown in Figure 6. The highest yield of HS^- was obtained for pH 5-6, with the yield decreasing significantly when the pH was greater than 7. Very little HS^- was observed when the pH was 9 or greater. The mechanism for the electrolysis with a reversible chemical reaction prior to reduction was solved by Bard and Solon [27]. Analysis of the data in Figure 6 by this theory showed that the yield of HS^- was proportional to the equilibrium concentration of bisulfite, given by Reaction 10.

$$HSO_3^- + H_2O \rightarrow SO_3^{2-} + H_3O^+ \quad K_{a,2} \qquad (10)$$

The solid lines in Figure 6 are the theoretical lines using the theory of Bard and Solon and a $K_{a,2}$ equal to 7.35 (literature value: 7.3).

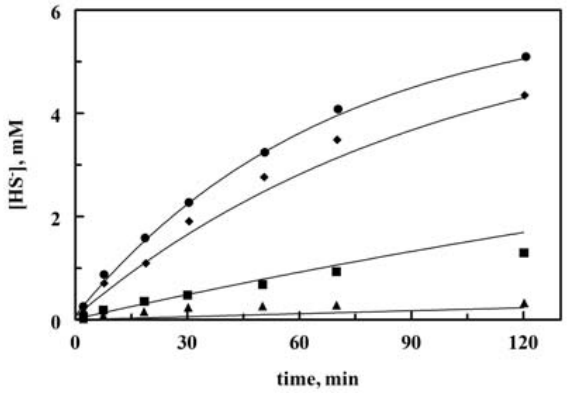

Fig. 6. Concentration of HS^- as a function of time and pH. pH 5 (●); pH 7 (♦); pH 8 (■); pH 9 (▲). Solid line based on the theory of Bard and Solon.

In order to probe this mechanism further, the coulometry of bisulfite at -600 mV (at the foot of the wave) were examined to determine if the new peak/shoulder led to different reduction products. At this potential, Fe^I was not formed. The electrolysis was carried out as above, taking aliquots of solution and determining the amount of HS^- generated. The current observed at -600 mV was substantially less than the current at -1100 mV, but it still decayed exponentially as expected for a controlled potential electrolysis. No HS^- was formed at -600 mV, regardless of pH. Under these conditions, bisulfite was nearly quantitatively converted to dithionite (98%).

$$HSO_3^- + H^+ + e^- \rightarrow \tfrac{1}{2}\, S_2O_4^{2-} + H_2O \qquad (11)$$

This potential does not correspond to either the Fe^{III} or Fe^{II} reduction potentials. It is not clear what the involvement of myoglobin/heme is in this reduction. This potential corresponds closely to the potential for the reduction of SO_2 to dithionite in non-aqueous solutions where SO_2 does not hydrate [28]. The myoglobin/heme was found to be necessary for the appearance of this wave, but it may only be involved in catalyzing the dehydration of bisulfite to SO_2, prior to reduction to dithionite, rather than the reduction of SO_2 itself.

If bisulfite can be reduced to dithionite at a potential positive of Fe^I, then the additional reduction products may involve a pathway through SO_2. In order to pursue this, the voltammetry and coulometry of dithionite was examined. At the Fe^{II}/Fe^I potential, it was found that dithionite could be reduced. Starting with dithionite, electrolysis was carried out at -1100 mV. As before, the current decayed exponentially, and the reduction product was found to be thiosulfate, which is consistent with previous work [29]. The thiosulfate was isolated from the electrolysis solution as the barium salt, and its identity verified by infrared spectrophotometry [30].

Strong bands confirmatory of thiosulfate were observed at 635, 1000 and 1100 cm^{-1}. The overall reduction of dithionite at -1100 mV is given by Eq. 11

3.2. Spectroelectrochemistry of bisulfite at Mb/DDAB Films

In order to better elucidate the reduction mechanism, the visible spectroelectrochemistry of bisulfite at Mb/DDAB films was undertaken. The electrolysis of the solution without bisulfite was carried out. During the voltammetric scan, the band for Fe(III)-Mb disappeared, and new bands for Fe(II)-Mb, and finally, Fe(I)-Mb appeared. With the addition of 20 mM bisulfite in buffered solutions containing 50 mM KBr as supporting electrolyte, spectra were recorded as a function of electrolysis time (Figure 7) at -1100 mV at pH 5. The most prominent band in the spectra was the band at 316 nm. This band increased initially during the electrolysis, before disappearing at the end of the electrolysis. This band was consistent with dithionite, which can be formed by the dimerization of $SO_2^{-\cdot}$ [31], which was also found above using chemical analysis of the electrolysis products.

At lower concentrations of bisulfite, a new band at 277 nm was observed, along with the 316 nm band. The 277 nm band was consistent with a charge transfer complex of the $SO_2^{-\cdot}$ with the ammonium ions in the film. The band has been observed by Eugene et al. [32], as well as other workers where the $SO_2^{-\cdot}$ species is generated [33], which was generated during the electrolysis.

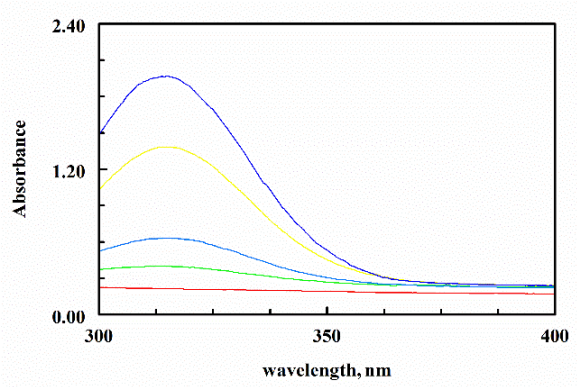

Fig. 7. UV-visible spectra during the electrolysis of 20 mM bisulfite at pH 5.0. Time: 0 min (red); 2 min (green); 4 min (blue); 10 min (yellow); 15 min (blue).

4. Conclusions.

Two waves in the voltammetry of bisulfite at a myoglobin/surfactant film are related to the presence of bisulfite. The first at -600 mV is due to the reduction of bisulfite.

$$Fe^{II}(P)\text{-}SO_3H + H^+ + e^- \rightarrow Fe^{II}(P) + SO^2\text{-}\cdot + H^2O \quad (13)$$

$$2\ SO_2 + 2\ e^- \rightarrow S_2O_4^{2-} \quad (14)$$

At this potential, only a single electron reduction of bisulfite is possible. The reduction could occur via a heme catalyzed dehydration of bisulfite or the direct reduction of iron coordinated bisulfite. Under more basic conditions, sulfite is coordinated to iron and is harder to reduce. In the absence of hemes, no reduction of bisulfite was observed at the surfactant film. These results are similar to iron porphyrin nitrosyl complexes where free and coordinated NO are reduced at similar potentials [34].

The second wave at -1100 mV involves the heme catalyzed multi-electron reduction of bisulfite to hydrogen sulfide, along with the reduction of bisulfite to dithionite. Based on the sulfite reductase mechanism, the reduction of bisulfite consists of a series of 2 e^-/2 H^+ steps which were followed by loss of water (Scheme 1). In this mechanism, the electrode potential would have maintained the iron in the Fe(I) state rather than the ferric state. With the reduction of the heme to Fe(I), a rapid two-electron reduction is possible which avoids the formation of $SO_2^{-\cdot}$ and dithionite. Unlike the formation of the SO_2^- radical, the oxysulfur species remained coordinated to the iron, allowing for the formation of HS^- in relatively large yields.

After the last electron transfer, sulfide will be released as H_2S/HS^-, and the catalyst will continue with the formation of a new Fe(I)-heme species. While the formation of HS^- was the major species at -1100 mV, the one-electron reduction of bisulfite still occurred, leading to dithionite. At this potential, the dithionite is reduced rapidly to thiosulfate, the rate of which was limited by the diffusion/convection rate.

References

[1] F. Grein, A. R. Ramos, S. S. Venceslau, I. A. C. Pereira, *Biochim. Biophys. Acta* **2013**, *1827*, 145-160.
[2] J. Simon, P. M. H. Kroneck, *Adv. Microb. Physiol.* **2013**, *62*, 45-117.
[3] B. R. Crane, L. M. Siegel, E. D. Getzoff, *Biochemistry* **1997**, *36*, 12120-12137.
[4] K. Parey, E. Warkentin, P. M. H. Kroneck, U. Ermler, *Biochemistry* **2010**, *49*, 8912-8921.
[5] J. Tan, J. A. Cowan, *Biochemistry* **1991**, *30*, 8910-8917.
[6] R. Silaghi-Dumitrescu, S. V. Makarov, *Int. J. Quantum Chem.* **2012**, *112*, 900-908.
[7] T. F. Oliveira, C. Vonrhein, P. M. Matias, S. S. Venceslau, I. A. C. Pereira, M. Archer, *J. Biol. Chem.* **2008**, *283*, 34141-34149.
[8] A. A. Santos, S. S. Venceslau, F. Grein, W. D. Leavitt, C. Dahl, D. T. Johnston, I. A. C. Pereira, *Science* **2015**, *350*, 1541-1545.
[9] R. Barbour, Z. G. Wang, I. T. Bae, Y. V. Tolmachev, D. A. Scherson, *Anal. Chem.* **1995**, *67*, 4024-4027.
[10] aE. Jacobsen, D. T. Sawyer, *J. Electroanal. Chem.* **1967**, *15*, 181-192; bC. S. Yu, H. Choi, S. Kim, *Chem. Lett.* **2002**, 648-649.
[11] M. A. Kline, M. H. Barley, T. J. Meyer, *Inorg. Chem.* **1987**, *26*, 2196-2197.
[12] W. R. Scheidt, Y. J. Lee, M. G. Finnegan, *Inorg. Chem.* **1988**, *27*, 4725-4730.
[13] M. S. Reynolds, R. H. Holm, *Inorg. Chim. Acta* **1989**, *155*, 113-123.
[14] T. Kuroi, K. Nakamoto, *J. Mol. Struct.* **1986**, *146*, 111-121.
[15] M. Massoudipour, S. K. Tewari, K. K. Pandey, *Polyhedron* **1989**, *8*, 1447-1451.
[16] J. F. Rusling, A. E. F. Nassar, *J. Am. Chem. Soc.* **1993**, *115*, 11891-11897.
[17] aM. T. De Groot, M. Merkx, M. T. M. Koper, *J. Am. Chem. Soc.* **2005**, *127*, 16224-16232; bM. T. De Groot, M. Merkx, M. T. M. Koper, *Electrochem. Commun.* **2006**, *8*, 999-1004.
[18] P. M. Guto, J. F. Rusling, *Electrochem. Commun.* **2006**, *8*, 455-459.
[19] T. Sagara, T. Sakai, H. Nagatani, *Electrochem. Commun.* **2007**, *9*, 2018-2022.
[20] C.-Y. Lee, A. M. Bond, *Langmuir* **2010**, *26*, 5243-5253.
[21] A. E. F. Nassar, J. M. Bobbitt, J. D. Stuart, J. F. Rusling, *J. Am. Chem. Soc.* **1995**, *117*, 1098610993.
[22] R. Lin, M. Bayachou, J. Greaves, P. J. Farmer, *J. Am. Chem. Soc.* **1997**, *119*, 12689-12690.
[23] S. M. Chen, C. C. Tseng, *Electrochim. Acta* **2004**, *49*, 1903-1914.
[24] A. P. H. Association, *Standard Methods for the Examination of Water and Wastewater*, 19th ed., Washington, DC, **1995**.
[25] E. Gasana, P. Westbroek, E. Temmerman, H. P. Thun, *Anal. Commun.* **1999**, *36*, 387-389.
[26] A. J. Bard, J. S. Mayell, *J. Phys. Chem.* **1962**, *66*, 2173-2179.
[27] A. J. Bard, E. Solon, *J. Phys. Chem.* **1963**, *67*, 2326-2330.
[28] R. W. Garber, C. E. Wilson, *Anal. Chem.* **1972**, *44*, 1357-1360.
[29] V. Cermak, M. Smutek, *Collect. Czech. Chem. Commun.* **1975**, *40*, 3241-3264.

[30] F. A. Miller, C. H. Wilkins, *Anal. Chem.* **1952**, *24*, 1253-1262.
[31] aF. Magno, G. A. Mazzocchin, G. Bontempelli,
J. Electroanal. Chem. **1974**, *57*, 89-96; bC. L. Gardner, D. T. Fouchard, W. R. Fawcett, *J. Electrochem. Soc.* **1981**, *128*, 2337-2345; cB. S. Kim, S. M. Park, *J. Electrochem. Soc.* **1993**, *140*, 115-122.
[32] F. Eugene, B. Langlois, E. Laurent, *New J. Chem.* **1993**, *17*, 815-821.
[33] J. Grundnes, S. D. Christian, *J. Am. Chem. Soc.* **1968**, *90*, 2239-2245.
[34] D. Lançon, K. M. Kadish, *J. Am. Chem. Soc.* **1983**, *105*, 5610-5617.

Supplementary Material

Sulfide-potentiometric determination method

Calibration curve

To 40.0 mL of buffer solutions (pH 5-9) containing 0.10 M KCl in order to maintain the ionic strength, 1 mL of a NaHS solution standard was added. The potential of the solutions was recorded in each buffer, using a sulfide-selective electrode together with a double-junction reference electrode that connected to a pH-meter with millivolt scale. The potential was measured after the values had stabilized. The electrodes were removed, rinsed and dried with a tissue and the next NaHS solution standard was measured. The potential as a function of the logarithm (to the base 10) of sulfide concentration was plotted for all buffers. The plot for sulfide standards in the Tris buffer (pH 7.3) is shown in Figure S1. The slope was -28.5□0.1 mV. The slope and the intercept were calculated from the linear portion of the calibration plot in each buffer and used to calculate the concentration of sulfide from the bisulfite electrolyses in different buffers (pH 5-9).

Figure S1. Calibration curve for HS- from standards pH 7.3 Tris buffer. 0.10 M KCl, 25°C.

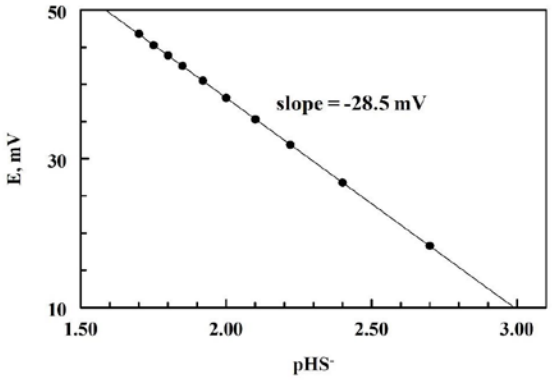

Sulfide determination

During the electrolysis of the bisulfite solutions in different buffers (pH 5-9) using the Mb-DDAB films, aliquots of the solutions were removed at fixed time intervals and added to 40.0 mL buffer solutions containing 0.1 M KCl to maintain the constant ionic strength. The potentials of the solutions were recorded after the values had stabilized. The concentration of sulfide in the electrolysis was obtained using the slopes and intercepts from the previously constructed calibration plots. A typical set of data at pH 7.3 is shown in Table S1.

Table S1. Typical set of electrolysis data for the coulometry of 20 mM bisulfite at pH 7.3

Time, min.	E, mV	[HS-], mV
2.0	10.4	0.97
4.0	10.9	1.47
6.0	11.6	2.25
10.	13.3	3.76

15.	14.9	5.12
20.	17.4	6.40
25	18.1	7.09
30	19.2	7.71
40	21.6	8.77
50	24.1	9.60
60	26.4	10.2
75	29.9	11.
90	33.6	11.5
120	40.6	12.2

Bisulfite-spectrophotometric determination method

a. Calibration curve

An absorbing solution was made by adding 5 mL 1,10-phenanthroline solution, 0.5 mL ferric ammonium sulfate solution, 25 mL distilled water, 5 drops octyl alcohol (to act as a defoamer) to a 100-mL Nessler tube. A gas dispersion tube was inserted. A 5.0 mL sample of the 20 mM $NaHSO_3$ standard solution and 1.0 mL sulfamic acid solution was added to the gas washing bottle. A 10.0 mL (1:1) HCl acid solution was then added and immediately connected the gas washing bottle which was connected tightly to the gas train using a spring or a rubber band to keep the top securely closed during the gas flow. Nitrogen gas flow rate was adjusted to 2.0 L/min and the solution was purged for 60 min (1hr). The same procedure was repeated for the other $NaHSO_3$ standards that bracket the sample (16, 14, 12, 10, 8, 6, 4, 2 and 0 mM $NaHSO_3$ standards, respectively).

After exactly one hour, the nitrogen flow was turned off, the Nessler tube was disconnected and immediately 1 mL ammonium bi-fluoride solution was added. The gas dispersion tube was removed, rinsed with distilled water, and the rinse water was forced into the Nessler tube with a rubber bulb. The solution was diluted to 50 mL in the same Nessler tube and mixed thoroughly by rapidly moving the tube in a circular motion. After exactly 5 minutes from the time of adding ammonium bi-fluoride, the absorbance was recorded versus distilled water at 510 nm using a 1 cm cell. A calibration curve of the $NaHSO_3$ standards concentration versus absorbance was plotted (Figure S2). The slope (7.3 x 10^{-3} mM^{-1}) and intercept were calculated together with their standard deviations (1.0 x 10^{-4} mM^{-1}), and were used to calculate the bisulfite concentrations during the electrolysis.

Figure S2. Calibration curve for the determination of bisulfite by the phenanthroline method.

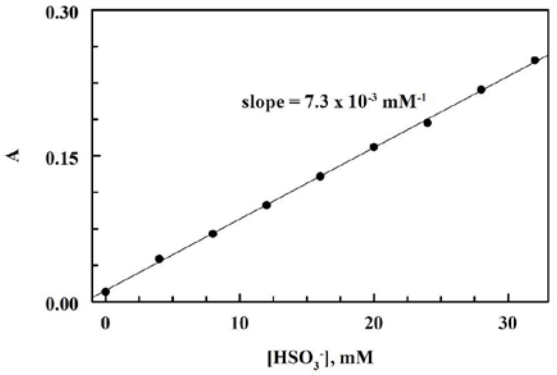

b. Bisulfite determination by comparison with calibration curve

During the electrolysis of bisulfite solution, aliquots of the solutions were removed at fixed time intervals, added to the SO_2 gas evolution apparatus, purged for 60 minutes using the same procedure for the $NaHSO_3$ standards and measured at 510 nm versus distilled water. The concentrations of the bisulfite corresponding to each time

interval in each buffer were obtained from the calibration plot using the value of slope and intercept together with their standard deviations.

Determination of dithionite using rotating disk voltammetry

Aliquots of dithionite standards were added to 0.10 M NaOH solutions. Linear sweep voltammograms (LSV) were obtained using a scan rate of 20 mV/s and a rotation rate of 1000 rpm. A wave for the oxidation of the dithionite produced during the electrolysis was observed (Figure S3). The limiting currents were measured and a calibration curve was constructed (Figure S4). Dithionite, LSV measurements were carried out on bisulfite solutions electrolyzed at various times using the same procedure. The dithionite concentration was determined from the calibration curve. A typical set of voltammograms for the oxidation of dithionite during the electrolysis at -600 mV is shown in Figure S5.

Figure S3. Linear sweep voltammograms at a uncoated glassy carbon rotating disk electrode (N = 1000 rpm) for the oxidation of dithionite standards (0, 2, 5, 10, 15, 20, and 25 mM) in alkaline solution (0.1 M NaOH, pH 12.5) at 20 mV/s.

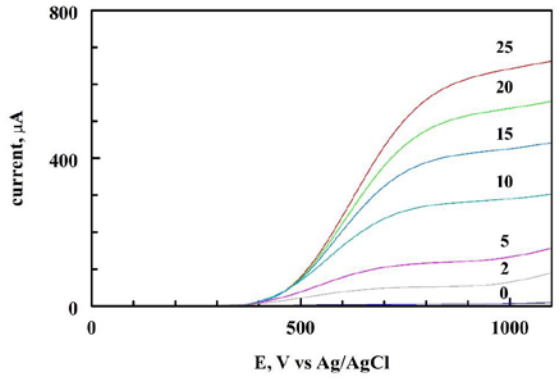

Figure S4. Calibration curve for dithionite using linear sweep voltammetry at a uncoated glassy carbon rotating disk electrode (rotation rate = 1000 rpm). The oxidation current of dithionite standards (0, 1, 2, 5, 10, 15, 20, and 25 mM) was measured at the limiting current in alkaline solution (0.1 M NaOH, pH 12.5) at 20 mV/s.

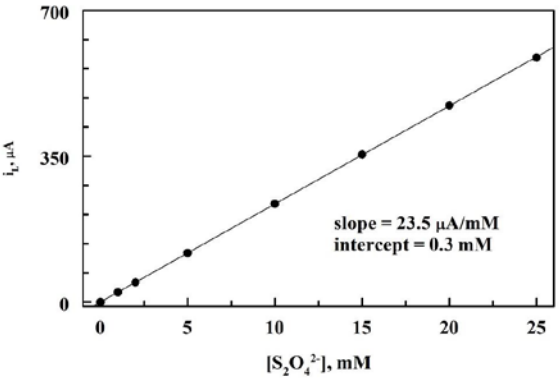

Figure S5. Linear sweep voltammograms at a uncoated glassy carbon rotating disk (rotation rate = 1000 rpm) electrode for dithionite produced at 2, 5, 15, 25, 30, 40, and 50 min during the electrolysis of 10.0 mM bisulfite in a pH 5 phthalate buffer solution containing 100 mM KBr at -600 mV using a Mb/DDAB film modified on a glassy carbon electrode.

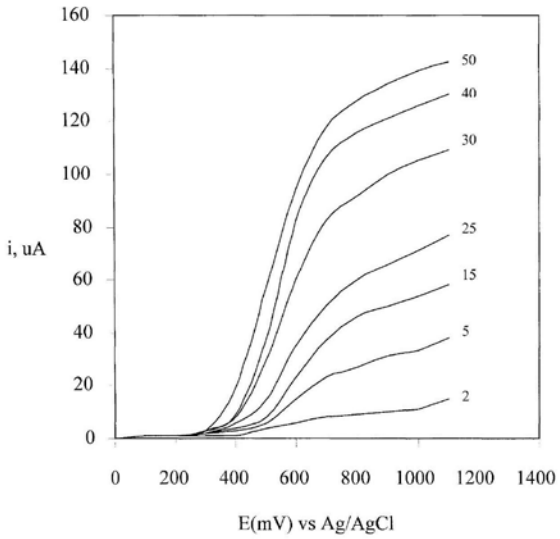
160
140
120
100
80
60
40
20
0
i, uA
0
200
400
600
800
1000
1200
1400
E(mV) vs Ag/AgCl
50
40
30
25
15
5
2